

Transforming Policy-Car Swerving for Mitigating Stop-and-Go Traffic Waves: A Practice-Oriented Jam-Absorption Driving Strategy

Zhengbing He

arXiv:2602.10234v2 [physics.soc-ph] 12 Feb 2026

Abstract—Stop-and-go traffic waves, as a major form of freeway traffic congestion, cause severe and long-lasting adverse effects, including reduced traffic efficiency, increased driving risks, and higher vehicle emissions. Amongst the freeway traffic management strategies, jam-absorption driving (JAD), in which a dedicated vehicle performs “slow-in” and “fast-out” maneuvers before being captured by a stop-and-go wave, has been proposed as a potential method for preventing the propagation of such waves. However, most existing JAD strategies remain impractical mainly due to the lack of discussion regarding implementation vehicles and operational conditions. Inspired by real-world observations of police-car swerving behavior, this paper first introduces a Single-Vehicle Double-Detector Jam-Absorption Driving (SD-JAD) problem, and then proposes a practical JAD strategy that transforms such behavior into a JAD strategy capable of suppressing the propagation of an isolated stop-and-go wave. Five key parameters that significantly affect the proposed strategy, namely, JAD speed, inflow traffic speed, wave width, wave speed, and in-wave speed, are identified and systematically analyzed. Using a SUMO-based simulation as an illustrative example, we further demonstrate how these parameters can be measured in practice with two stationary roadside traffic detectors available. The results show that the proposed JAD strategy successfully suppresses the propagation of a stop-and-go wave, particularly with no secondary waves triggered. This paper is expected to take a significant step toward making JAD practical, advancing it from a theoretical concept to a feasible and implementable strategy. To promote reproducibility in the transportation domain, we have also open-sourced all the code on our GitHub repository (<https://github.com/gotrafficgo>).

Index Terms—Traffic congestion, traffic control, travel time, vehicle dynamics, mobility, connected and automated vehicle

I. INTRODUCTION

STOP-AND-GO traffic waves (also referred to as wide moving jams or traffic oscillations) are a common form of traffic congestion on freeways. Such a freeway traffic pattern forces vehicles to repeatedly accelerate and decelerate, resulting in reduced traffic efficiency, longer travel times [1], [2], higher fuel consumption and emissions [3], [4], and an increased risk of traffic accidents [5], [6]. Even worse, such stop-and-go structures can propagate and sustain themselves over tens of kilometers under sufficiently high traffic demand, which further exacerbates their negative impacts.

Amongst the freeway traffic management strategies, jam-absorption driving (JAD), in which a dedicated vehicle performs “slow-in” and “fast-out” maneuvers before being cap-

tured by a stop-and-go wave, has been proposed as a potential method for preventing the propagation of such waves [7], [8]. Early studies focused on theoretical questions: Can JAD suppress stop-and-go waves? And will secondary waves be triggered? Initial analyses, based on the Kinematic Wave Theory and the Fundamental Diagram, concluded that JAD is effective [9]. Microscopic models such as the Helly car-following model and the Intelligent Driver Model were used to trace vehicle dynamics more explicitly [10], [11], though their conclusions rely on strong model assumptions. From 2017 onward, more practical, implementation-oriented JAD strategies have been proposed [12]. Core tasks include determining when to activate and deactivate a JAD vehicle and selecting the appropriate vehicle. The following works have incorporated wave propagation prediction [12], influential subspace concepts [13], capacity-drop considerations [14], multiple-wave suppression [15], and traffic efficiency and safety optimization [14], [16], [17]. Simulation is typically employed to demonstrate how JAD vehicles can effectively increase flow and suppress waves. For a more detailed introduction and discussion of recent JAD progress, one may refer to our latest review article [18].

Generally speaking, although JAD strategies have been extensively studied, most assume the availability of Connected and Automated Vehicles (CAVs) to perform JAD tasks and full access to traffic information to determine a specific JAD plan. Unfortunately, even with the rapid development of CAV technology, fully controlling one or a few CAVs in real-world traffic to implement actual traffic management remains highly challenging and rarely seen. Moreover, the issue of JAD triggering secondary waves has been raised in nearly all existing studies, yet few have actually addressed it. Therefore, while JAD is theoretically appealing, its practical implementation is still far from realization.

Occasionally, we observed a type of police-car swerving behavior frequently appearing on social media. As shown in Figure 1 and the footage in [19], a police car was recorded maneuvering at high speed across all lanes on a freeway in California, USA, to control the following traffic. Although the police car’s goal was still unclear to the authors (not jam absorption at least, we believe), this real-world behavior demonstrates the practical feasibility of deploying a slow-moving vehicle to moderate the speed of inflow.

Building on this real-world observation, this paper aims to develop a practically feasible strategy for suppressing stop-and-go waves. To this end, we formulate a *Single-Vehicle Double-Detector Jam-Absorption Driving (SD-JAD)* problem,



Fig. 1. Police-car swerving at high speed on a freeway, California, USA (Snapshots from the footage in [19]).

in which only two stationary roadside traffic detectors (upstream and downstream) and a single JAD vehicle are assumed to be available. Under these minimal conditions, the JAD objective is to block the propagation of a stop-and-go wave, specifically an isolated wave, which is distinct from the periodic stop-and-go waves associated with fixed-location bottlenecks.

We further propose a corresponding JAD strategy and identify five key parameters that significantly influence its performance, namely, *JAD speed*, *inflow traffic speed*, *wave width*, *wave speed*, and *in-wave speed*. The effects of these parameters on the strategy are thoroughly analyzed. Using SUMO-based simulation, we discuss how these parameters can be measured in practice with only two stationary traffic detectors, and demonstrate the effectiveness of the proposed JAD strategy. The triggering of secondary waves is successfully prevented by taking traffic stability into account when selecting the JAD speed. By leveraging police-car swerving behavior to implement JAD, we believe this work substantially advances JAD from a purely theoretical concept toward practical application. Moreover, to promote reproducibility in the transportation domain, we have open-sourced all the code on our GitHub repository (<https://github.com/gotrafficgo>).

The remainder of the paper is organized as follows. Section II introduces the SD-JAD problem. Section III proposes the JAD strategy and provides solutions to several key questions. Section IV presents a thorough theoretical analysis of the key parameters and demonstrates the results with numerical experiments. Section V uses a SUMO-based simulation to illustrate how these parameters can be measured in practice with only two stationary roadside traffic detectors and to validate the effectiveness of the proposed strategy. Finally, conclusions are drawn in Section VI.

II. PROBLEM STATEMENT

Inspired by the real-world observation of police-car swerving on the freeway in Figure 1 and the footage in [19], we introduce an SD-JAD problem as follows.

Definition 1. Single-Vehicle Double-Detector Jam-Absorption Driving (SD-JAD)

It is a freeway traffic control problem in which only a single dedicated vehicle is employed to suppress

the propagation of an upcoming isolated stop-and-go wave. The dedicated vehicle merges into the traffic stream from a fixed location (e.g., freeway shoulder or on-ramp), and both the dispatch decision and the detailed driving plan are determined solely based on information from a pair of detectors at upstream and downstream.

Note that the targeted stop-and-go wave is an isolated wave with high-density free-flow conditions both upstream and downstream. Such waves may originate from disturbances under high traffic density. Many existing variable speed limit (VSL) strategies, such as the well-known SPECIALIST [20], [21], are designed to address these types of waves [18]. In contrast, the proposed strategy does not aim to resolve periodic stop-and-go waves associated with a fixed-location bottleneck. Many existing JAD studies seem not carefully clarify this.

Figure 2 describes the problem, in which x_A denotes the location of the stand-by dedicated vehicle for JAD; x_d and x_u are the locations of the downstream and upstream detectors, respectively; w denotes the stop-and-go wave speed; v_t and v^* are the car-following speed and the pre-determined JAD speed of the JAD vehicle, respectively.

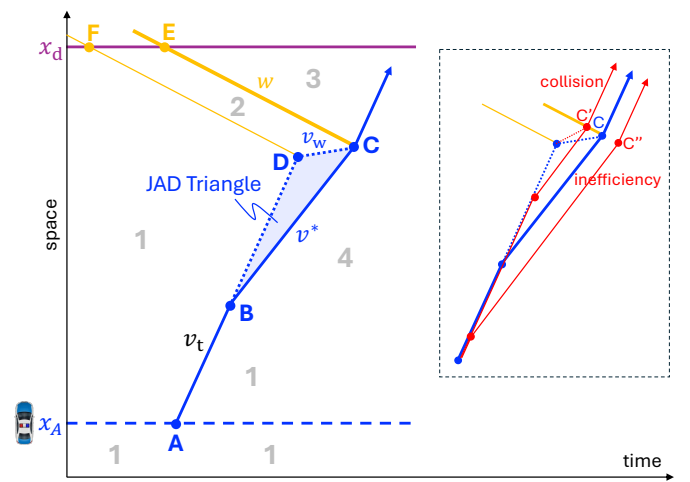


Fig. 2. A schematic diagram of the single-vehicle double-detector jam-absorption driving. Note the numbers in grey indicate traffic states.

There are a total of 6 critical time-space points:

- $A(t_A, x_A)$ is the point where the JAD vehicle enters traffic stream;
- $B(t_B, x_B)$ is the point where the JAD vehicle starts to implement the JAD task with the JAD speed v^* ;
- $C(t_C, x_C)$ is the point where the JAD vehicle stops to implement the JAD task, i.e., where the stop-and-go wave is terminated;
- $D(t_D, x_D)$ is the point where the JAD vehicle (or a regular vehicle) will reach the front of the stop-and-go wave without JAD intervention;
- $E(t_E, x_E)$ is the point where the temporal back of a stop-and-go wave is detected by the downstream detector at location x_d .
- $F(t_F, x_F)$ is the point where the temporal front of a stop-and-go wave is detected by the downstream detector at location x_d .

The JAD plan can be described as follows:

$$A \xrightarrow{v_t} B \xrightarrow{v^*} C, \quad (1)$$

where $A \xrightarrow{v_t} B$ is a process of floating within traffic and waiting for an appropriate moment and $B \xrightarrow{v^*} C$ is the actual JAD process.

We also define the triangle BCD as the **JAD Triangle**, which directly determines the details of a JAD strategy. The common condition for the JAD Triangle is

$$v_t > v^* > v_w \geq 0. \quad (2)$$

Points E and F are associated with the stop-and-go wave detected by the downstream detector at x_d , and thus $x_d = x_E = x_F$. The temporal width of the stop-and-go wave can be denoted by $\Delta_w = t_E - t_F$.

The key questions to solve the SD-JAD problem are as follows.

- Q1. What is the JAD speed, i.e., v_A ?
- Q2. What is the JAD plan, i.e., $A \xrightarrow{v_t} B \xrightarrow{v^*} C$?

It is worth noting that terminating the JAD task earlier or later than point C (e.g., at C' or C'') will lead to danger or inefficiency, as shown in Figure 2.

The key assumptions are as follows.

- A1. Stop-and-go waves propagate backward at an approximately constant speed, which is quite consistent with real-world observations [22]–[26].
- A2. The length of the backward-moving queue is also approximately constant, instead of continuously increasing, as shown in the real-world observations such as those in Figure ???. If the queue can shrink itself (e.g., due to the inflow decrease), there is no need to dispatch a JAD vehicle. This assumption can be relaxed by incorporating other information to estimate the changes of wave width.
- A3. For simplicity, we assume an instantaneous speed change in the theoretical analysis. In simulation or practice, a gradually-changing speed would not largely change the results, as shown in [12].

III. KEY QUESTIONS AND SOLUTIONS

A. Q1: What is the JAD speed?

First, the JAD speed should be lower than the speed of the surrounding or upcoming traffic, i.e., $v^* < v_t$, according to the original “slow-in” and “fast-out” idea of JAD.

Second, as extensively discussed in [18], the main possible hazard of JAD is the triggering of secondary waves. Therefore, avoiding the triggering of secondary waves is the main consideration in determining the JAD speed.

According to fundamental traffic flow theory, secondary waves or traffic breakdowns are primarily associated with traffic instability. Generally speaking, the low density is stable while the high density is easy to break down¹ (Figure 3). There might be a critical density (denoted by k') and the associated critical speed (denoted by v'), which separates the states². Therefore, to avoid triggering the secondary wave, the JAD speed should be higher than the critical speed, i.e., $v^* \geq v'$.

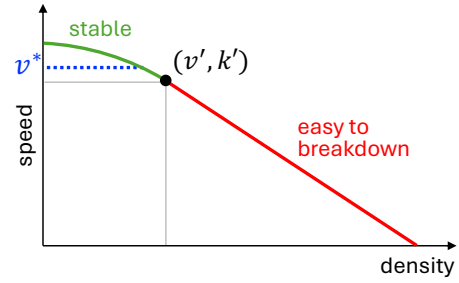


Fig. 3. The speed-density relationship and traffic instability. v' and k' denote the critical traffic state, separating stable and unstable traffic states.

Unfortunately, determining the value of v' for real-world traffic remains challenging, even though it is well understood that traffic instability is directly related to human drivers' imperfections and can be explained using traffic stability theory. The main difficulty arises from the heterogeneity of traffic, including both vehicle and driver behavior heterogeneity, which is highly complex and dynamic, making accurate measurement of v' in real traffic extremely challenging. In this paper, as we will show later, we determine the value using simulation. In practice, one could select a conservative value for v^* , i.e., a value relatively higher than the assumed v' based on experience, which would greatly simplify the problem. This is a problem that cannot be fully addressed in a single paper, and thus more in-depth study on this estimation of v' is expected.

B. Q2: What is the JAD plan? Part I: Points B and C

As shown in Figure 2, the JAD plan can be described as (1). We assume that the values of the following variables have

¹The notion of stability can differ depending on the perspective. From a microscopic or dynamical viewpoint, a high-density flow is linearly unstable, i.e., small perturbations can grow into stop-and-go waves. However, from a macroscopic or phase perspective, once traffic has already entered a congested state, the flow pattern becomes relatively stable and does not further break down. In this study, the instability we refer to is of the first type, i.e., from a microscopic viewpoint.

²The critical density and speed here may differ from those commonly used in traffic flow theory to separate free-flow and congested conditions.

been pre-determined:

- The pre-defined JAD speed v^* ,
- The surrounding or upcoming traffic speed v_t ,
- The temporal back and front of a stop-and-go wave at a fixed location, detected by the downstream detector at x_d , i.e., points E and F ,
- The wave speed w .

The selection of point A will be carefully discussed later in Section III-C. Here, we simply assume that point A is known, and then we only need to measure points B and C . Referring to Figure 2, from a geometric perspective, given point F and slope w , we have line DF expressed as follows:

$$DF : x = x_F + w(t - t_F). \quad (3)$$

Given point E and slope w , we have line CE expressed as follows:

$$CE : x = x_E + w(t - t_E). \quad (4)$$

Given point A and slope v_t , we have line AD expressed as follows:

$$AD : x = x_A + v_t(t - t_A). \quad (5)$$

From lines DF and AD , we can obtain the intersection D as follows:

$$D(A, F, v_t, w) : \begin{cases} t_D = \frac{v_t t_A - w t_F + (x_F - x_A)}{v_t - w}, \\ x_D = x_A + v_t(t_D - t_A). \end{cases} \quad (6)$$

Given point D and slope v_w , we have line CD expressed as follows:

$$CD : x = x_D + v_w(t - t_D). \quad (7)$$

From lines CD and CE , we can obtain the intersection C as follows:

$$C(D, E, v_w, w) : \begin{cases} t_C = \frac{v_w t_D - w t_E + (x_E - x_D)}{v_w - w}, \\ x_C = x_D + v_w(t_C - t_D). \end{cases} \quad (8)$$

Given point C and slope v^* , we have line BC expressed as follows:

$$BC : x = x_C + v^*(t - t_C). \quad (9)$$

Given point A and slope v_t , we have line AB expressed as follows:

$$AB : x = x_A + v_t(t - t_A). \quad (10)$$

From lines BC and AB , we can obtain the intersection B as follows:

$$B(A, C, v_t, v^*) : \begin{cases} t_B = \frac{v_t t_A - v^* t_C + (x_C - x_A)}{v_t - v^*}, \\ x_B = x_A + v_t(t_B - t_A). \end{cases} \quad (11)$$

Finally, we have the JAD plan $A \xrightarrow{v_t} B \xrightarrow{v^*} C$.

C. Q2: What is the JAD plan? Part II: Point A

In practice, the location and moment (i.e., point A) to dispatch a JAD vehicle may be determined by traffic managers. Specifically, a JAD vehicle initially stands by at a fixed roadside location or an on-ramp, denoted by x_A . Once a downstream stop-and-go wave is confirmed to be developing, the JAD vehicle is dispatched at time t_A , subject to practical considerations such as the emergence of a sufficiently large traffic gap. However, this appointment is also constrained by a feasible range of points A , and this subsection focuses on determining the feasible range of the starting point A .

With the aid of Figure 4, we analyze the feasible region of point A . We begin by ignoring point A^3 and considering the JAD Triangle BCD , whose sides BC , BD , and CD have fixed slopes v^* , v_t , and v_w , respectively. Points C and D are constrained to lie on the parallel lines CE and DF , both with slope w . Since the shape of the JAD Triangle BCD is fixed and segment CD is confined between these two parallel lines, the JAD Triangle BCD can only undergo rigid translations along a direction with slope w , under which point B traces a straight line, denoted by ℓ , with slope w .

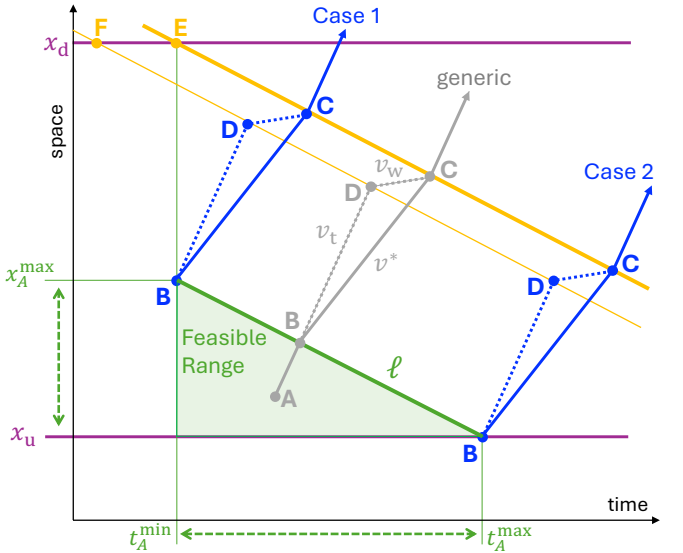


Fig. 4. Feasible region of the dispatch time and location (point A) of a JAD vehicle.

We have the following conditions. Points C lies on lines CE in (4) and line BC in (9), giving

$$x_C = x_E + w(t_C - t_E), \quad (12)$$

$$x_C = x_B + v^*(t_C - t_B). \quad (13)$$

Points D lies on line DF in (3) and line BD , giving

$$x_D = x_F + w(t_D - t_F), \quad (14)$$

$$x_D = x_B + v_t(t_D - t_B). \quad (15)$$

³In Section III-C, point A is assumed to be known, and the corresponding JAD plan is then constructed. This sequence is consistent with the natural decision-making process in practice, where a JAD opportunity is first identified and subsequently planned. Here, however, in order to characterize the feasible region of point A , we do not assume that point A is known a priori.

The slope of segment CD is

$$\frac{x_C - x_D}{t_C - t_D} = v_w, \quad (16)$$

and, as shown in Figure 4, the geometric relations among the points are as follows,

$$\begin{aligned} t_F &< t_E < t_D < t_C, \\ x_D &< x_C < x_E = x_F, \\ 0 \leq v_w &< v^* < v_t, \\ 0 &> w. \end{aligned} \quad (17)$$

Combining (12)–(17), we can derive the trajectory of point B as

$$x_B = x_E + w(t_B - t_E) + \frac{w\Delta_w(v_t - v_w)(w - v^*)}{(w - v_w)(v_t - v^*)}. \quad (18)$$

From a reactive perspective (i.e., without prediction), a JAD vehicle can be dispatched only after the formation of a stop-and-go wave is confirmed at time t_E ($t_E > t_F$); see Case 1 in Figure 4. The upstream detector located at x_u defines the farthest admissible stand-by location of the JAD vehicle; see Case 2 in Figure 4. Therefore, the temporal and spatial lower bounds are given as follows:

$$t_B \geq t_E, \quad x_B \geq x_u. \quad (19)$$

The feasible region of point B is then the portion of line ℓ that lies within these bounds.

Substituting the bounds in (19) into line ℓ in (18), three intersection points are obtained, namely

$$(t_{\min}, x_{\max}), \quad (t_{\min}, x_{\min}), \quad (t_{\max}, x_{\min}).$$

These three points form a triangle, which defines the feasible region of point A , since point A is the backward extension of point B along the space-time direction.

IV. THEORETICAL ANALYSIS OF THE JAD

Segment BC represents a JAD process with distance J_{dis} and duration J_{dur} . Given two parallel lines CE in (4), ℓ in (18), and the geometric relations in (17), the spatial and temporal length of the segment BC , which is an in-between segment with slope v^* , can be written as follows:

$$\begin{aligned} J_{\text{dis}}(v^*, v_t, \Delta_w, w, v_w) &= x_C - x_B \\ &= -\frac{v^* w \Delta_w (v_t - v_w)(w - v^*)}{(v^* - w)(w - v_w)(v_t - v^*)}, \end{aligned} \quad (20)$$

$$J_{\text{dur}}(\Delta_w, w, v_t, v_w, v^*) = t_C - t_B = \frac{J_{\text{dis}}}{v^*}. \quad (21)$$

J_{dis} and J_{dur} are linearly related through distance-time-speed relationship, and are determined by five parameters, i.e., v^* , v_t , Δ_w , w , v_w . Therefore, analyzing the impact of the parameters on J_{dis} is sufficient to characterize the behavior of the JAD process, without loss of generality.

To facilitate the interpretation of the theoretical results, we summarize empirically plausible parameter ranges related to stop-and-go waves and JAD vehicles in Table I. These values are consistent with real-world traffic observations and serve as practical references for the subsequent analysis of the impact of various factors on JAD implementation.

A. Impact of JAD Speed

To analyze the impact of the JAD speed on the JAD process, we take the partial derivative of (20) with respect to v^* :

$$\frac{\partial J_{\text{dis}}}{\partial v^*} = \frac{w \Delta_w (v_t - v_w) v_t}{(w - v_w)(v_t - v^*)^2}. \quad (22)$$

Considering the geometric relations in (17), we have $w - v_w < 0$, and it follows that $\partial J_{\text{dis}}/\partial v^* > 0$, which indicates that the JAD distance increases monotonically with the JAD speed.

Physically, as illustrated in Figure 5, this implies that, with all other variables held constant, executing a JAD at a higher target speed v^* requires a longer distance to adequately interact with the stop-and-go traffic wave.

The nonlinear dependence of J_{dis} on v^* is governed by the squared denominator $(v_t - v^*)^2$. As v^* approaches v_t , the denominator tends to zero and the marginal increase $\partial J_{\text{dis}}/\partial v^*$ grows rapidly. This indicates that the JAD distance becomes increasingly sensitive to the target speed at higher v^* , i.e., a convex dependence of the JAD distance on the target speed, also illustrated in Figure 5. Therefore, planning a high JAD speed requires substantially longer execution distance.

A rough estimate using typical parameter ranges from Table I shows that $\partial J_{\text{dis}}/\partial v^*$ is on the order of $10^1 \sim 10^2$ m, which corresponds to a JAD duration on the order of $10^2 \sim 10^3$ s. This implies that an increase of 1 km/h in the JAD speed may require an additional 10~100 m of execution distance. The results of the numerical simulations shown in Figure 5 indicate that J_{dis} ranges from approximately 2 km to more than 12 km and J_{dur} ranges from approximately 50 s to more than 160 s, given moderate values of other parameters.

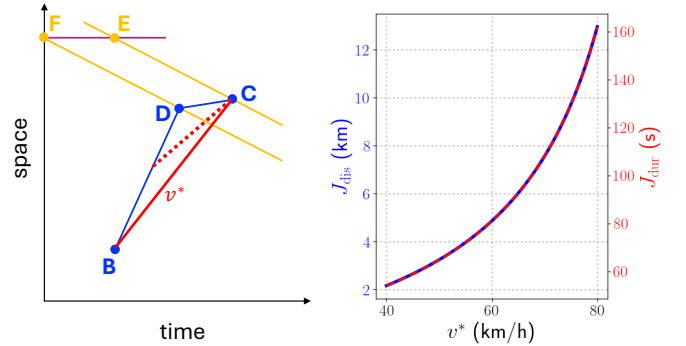


Fig. 5. The impact of JAD speed v^* on the JAD process (J_{dis} and J_{dur}). Left: schematic diagram; Right: results of numerical simulation, measured by keeping all other parameters at their midpoint values in Table I.

B. Impact of Inflow Traffic Speed

Likewise, from (20) the partial derivative of the JAD distance with respect to v_t can be written as follows:

$$\frac{\partial J_{\text{dis}}}{\partial v_t} = \frac{v^* w \Delta_w (w - v^*) (v^* - v_w)}{(v^* - w)(w - v_w)(v_t - v^*)^2}. \quad (23)$$

Considering the geometric relations in (17), we have that $\partial J_{\text{dis}}/\partial v_t < 0$, indicating that a higher inflow traffic speed reduces the required JAD distance.

TABLE I
PARAMETER RANGES RELATED TO STOP-AND-GO TRAFFIC WAVES AND JAD STRATEGIES

Parameter	Min	Max	Unit	Description
JAD speed (v^*)	40	80	km/h	Desired JAD speed that may not trigger secondary waves, considering traffic flow stability
Inflow traffic speed (v_t)	80	120	km/h	Speed of traffic approaching the stop-and-go traffic wave from upstream
Wave temporal width (Δ_w)	20	100	s	Temporal width of the stop-and-go traffic wave
Wave speed (w)	-20	-10	km/h	Wave speed of the stop-and-go traffic wave propagating upstream
In-wave speed (v_w)	0	20	km/h	Traffic speed inside the moving queue associated with the stop-and-go traffic wave

Physically, as illustrated in Figure 6, a faster inflow (red dashed line) results in a shorter distance and a shorter duration of the JAD process, under the constraint that all other variables are held constant. The nonlinear dependence of J_{dis} on v_t is dominated by the inverse-square term $(v_t - v^*)^{-2}$ in (23), implying the marginal reduction diminishes as v_t increases.

A rough order-of-magnitude estimate based on typical parameter ranges in Table I indicates that $\partial J_{\text{dis}}/\partial v_t$ is on the order of $10^1 \sim 10^2$ m, which corresponds to J_{dur} on the order of $10^1 \sim 10^2$ s. The results of the numerical simulations shown in Figure 5 indicate that J_{dis} ranges from approximately 4 to 7.5 km and J_{dur} ranges from approximately 60 to 130 s, given moderate values of other parameters.

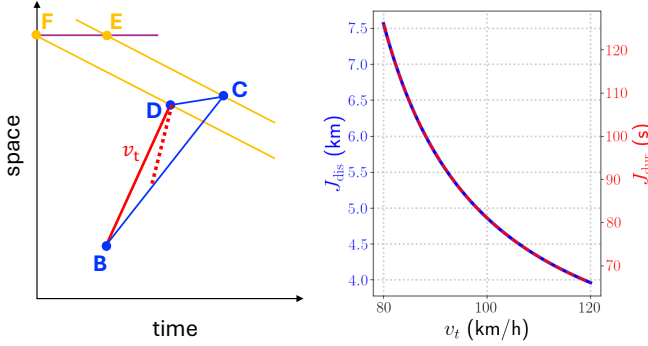


Fig. 6. The impact of inflow traffic speed v_t on the JAD process (J_{dis} and J_{dur}). Left: schematic diagram; Right: results of numerical simulation, measured by keeping all other parameters at their midpoint values in Table I.

C. Impact of Wave Temporal Width

From (20), the partial derivative of the JAD distance with respect to the wave width is

$$\frac{\partial J_{\text{dis}}}{\partial \Delta_w} = \frac{v^* w (v_t - v_w)}{(w - v_w)(v_t - v^*)}. \quad (24)$$

Considering the geometric relations in (17), we have that $\partial J_{\text{dis}}/\partial \Delta_w > 0$, indicating that wider waves require longer JAD distances.

Physically, a longer-lasting stop-and-go wave demands that the JAD vehicle travel a greater distance to fully interact with the moving queue (Figure 7).

The dependence is linear in the wave width Δ_w , which is also confirmed by the numerical simulation shown in Figure 7. It can be seen from the theoretical analysis in the left subfigure of Figure 7, an increase in Δ_w leads to a proportional expansion of the JAD Triangle BCD .

Increasing the wave duration from its lower to upper bound in Table I typically increases J_{dis} by an order of $10^1 \sim 10^2$ m, corresponding to J_{dur} on the order of $10^1 \sim 10^2$ s. The simulation results in Figure 7 further indicate that, for moderate values of the other parameters, J_{dis} ranges from approximately 2 to 8 km, and J_{dur} ranges from approximately 30 to 140 s.

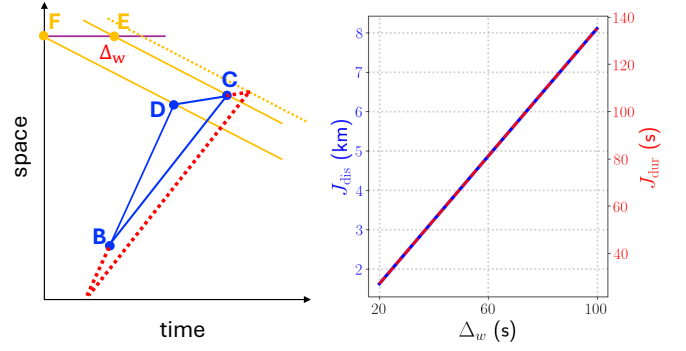


Fig. 7. The impact of wave width Δ_w on the JAD process (J_{dis} and J_{dur}). Left: schematic diagram; Right: results of numerical simulation, measured by keeping all other parameters at their midpoint values in Table I.

D. Impact of Wave Speed

From (20), the partial derivative of the JAD distance with respect to the wave speed is given by

$$\frac{\partial J_{\text{dis}}}{\partial w} = -\frac{\Delta_w, v^*, v_w (v_t - v_w)}{(v_t - v^*)(w - v_w)^2}. \quad (25)$$

Considering the geometric relations in (17), all terms in the denominator are positive, and the numerator is also positive except for the leading minus sign. Hence, $\partial J_{\text{dis}}/\partial w < 0$. Since $w < 0$, an increase in w (i.e., a reduction in its magnitude) corresponds to a slower propagation of the stop-and-go wave. Therefore, a slower wave speed leads to a shorter required JAD distance and duration (Figure 8).

As shown in (25), the sensitivity of J_{dis} to w scales with $(w - v_w)^{-2}$, implying a rapid change in the required JAD distance as the assumed wave speed approaches the actual propagation speed of the stop-and-go wave. This nonlinear amplification effect is clearly illustrated by the numerical results in Figure 8.

Varying the wave speed within the range reported in Table I typically leads to changes in J_{dis} on the order of $10^2 \sim 10^3$ m, and in J_{dur} on the order of $10^1 \sim 10^2$ s. The simulation results in Figure 8 further show that, for moderate values of the other parameters, the range of J_{dis} is between 4 and 5.4 km, and

the range of J_{dur} is between 65 and 90 s. Compared with the ranges resulted by other parameters, the wave speed's impact on the JAD process is relatively small.

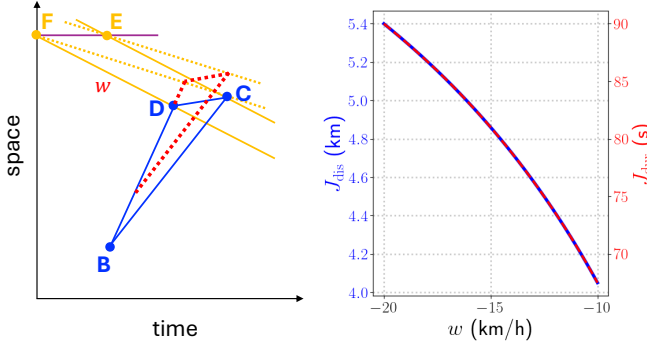


Fig. 8. The impact of wave width w on the JAD process (J_{dis} and J_{dur}). Left: schematic diagram; Right: results of numerical simulation, measured by keeping all other parameters at their midpoint values in Table I.

E. Impact of In-Wave Traffic Speed

From (20), the partial derivative of the JAD distance with respect to v_w is

$$\frac{\partial J_{\text{dis}}}{\partial v_w} = \frac{v^* w \Delta_w (v_t - w)}{(v_t - v^*)(w - v_w)^2}. \quad (26)$$

Considering the geometric relations in (17), we have that $\partial J_{\text{dis}} / \partial v_w < 0$, indicating that higher in-wave traffic speed reduces the required JAD distance.

Physically, when the vehicles inside the stop-and-go wave move faster, the JAD Triangle becomes smaller, and the JAD process is shortened accordingly. This means that, compared with a stop-and-go wave, a slow-moving-and-go wave is easier to mitigate, which is consistent with the common sense.

The nonlinear dependence on v_w is reflected in the squared term $(w - v_w)^2$ in the denominator. For typical values of v_w in the range 0~20 km/h, variations in J_{dis} are moderate on the order of $10^1 \sim 10^2$ m, corresponding to J_{dur} on the order of $10^2 \sim 10^3$ s. The simulation results in Figure 9 further show that, for moderate values of the other parameters, the range of J_{dis} is between 3 km and 9 km, and the range of J_{dur} is between 60 s and 150 s.

F. Summary of Parameter Sensitivity

Based on the preceding theoretical analysis, the sensitivity of the JAD implementation to key parameters can be summarized as follows, as shown in Table II.

- The impacts of JAD speed v^* and wave width Δ_w on J_{dis} and J_{dur} are positive, i.e., higher v^* and larger Δ_w lead to a longer JAD process, while fixing all other parameters.
- The impacts of inflow traffic speed v_t , wave speed w , and in-jam traffic speed v_w on J_{dis} and J_{dur} are negative, indicating that a lower v_t , a faster propagating wave (smaller $|w|$), and lower v_w require a longer JAD process.
- All the impacts are nonlinear, except for that of the wave width Δ_w , which is linear.

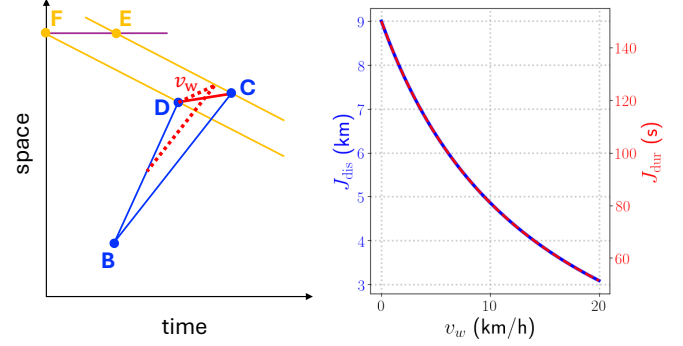


Fig. 9. The impact of in-wave traffic speed Δ_w on the JAD process (J_{dis} and J_{dur}). Left: schematic diagram; Right: results of numerical simulation, measured by keeping all other parameters at their midpoint values in Table I.

TABLE II
SUMMARY OF PARAMETER INFLUENCE ON JAD IMPLEMENTATION

Impact Ranking	Parameter	Direction	J_{dis} (km)	J_{dur} (s)
1	JAD speed (v^*)	+	[2, 13]	[50, 160]
2	Wave width (Δ_w)	+	[1, 8]	[30, 140]
3	Wave speed (w)	-	[3, 9]	[50, 150]
4	Inflow speed (v_t)	-	[4, 7.5]	[60, 130]
5	In-wave speed (v_w)	-	[4, 5.4]	[60, 90]

Note: “+” (“-”) indicates that the parameter increases (decreases) the corresponding JAD quantity.

- Considering the moderate values of the other parameters, the relative influence of each parameter on J_{dis} and J_{dur} , from strongest to weakest, is:

$$v^* > \Delta_w > v_w > v_t > w,$$

and the corresponding ranges are listed in Table II.

Referring to real-world scenarios, such temporal and spatial requirements are within the operational capabilities of JAD vehicles, including police cars that exhibit the observed swerving behavior, implying that the proposed JAD strategy is feasible and implementable under typical traffic conditions.

V. SIMULATION-BASED ANALYSIS AND PRACTICAL SETTING DEMONSTRATION

A. Simulation Scenario

It is known that speed variance between lanes is usually small, as lane-changing behavior tends to smooth out inter-lane differences [27]–[29]. Therefore, single-lane traffic or the average across all lanes is representative of multi-lane traffic. Without loss of generality, we simulate traffic on a single-lane straight freeway. SUMO is employed to simplify reproducibility. The road length is 8 km, with a speed limit of 90 km/h. The simulation runs for 1600 s with a time step of 1 s. Vehicles enter the network at the freeway entrance every 1.5 s⁴ with an initial speed of 54 km/h, and they soon accelerate

⁴Such a persistently high demand is effective in ensuring the continuous growth of a stop-and-go wave. We also experimented with more stochastic demand patterns, but failed to produce a self-sustaining wave.

to their maximum speed. The Krauss car-following model embedded in SUMO is employed, and the main parameters are summarized in Table III.

TABLE III
MAIN PARAMETERS OF THE KRAUSS MODEL

Parameter	Value	Unit
Max Acceleration	2.0	m/s^2
Max Deceleration	4.5	m/s^2
Desired Reaction Time	1.2	s
Reaction Time Variation	1.2	s
Acceleration Variation	0.95	—
Deceleration Variation	0.95	—
Driver Randomness	0.95	—
Vehicle Length	5	m
Minimum Gap	1.5	m
Max Speed	25	m/s
Speed Factor	1.0	—
Speed Deviation	0.0	—

To test the JAD strategy, a disturbance is artificially introduced by stopping the first vehicle in the simulation 500 m before the end of the road for 30 s. This generates a clear and self-sustaining stop-and-go wave that propagates upstream and does not dissipate on its own (Figure 10).

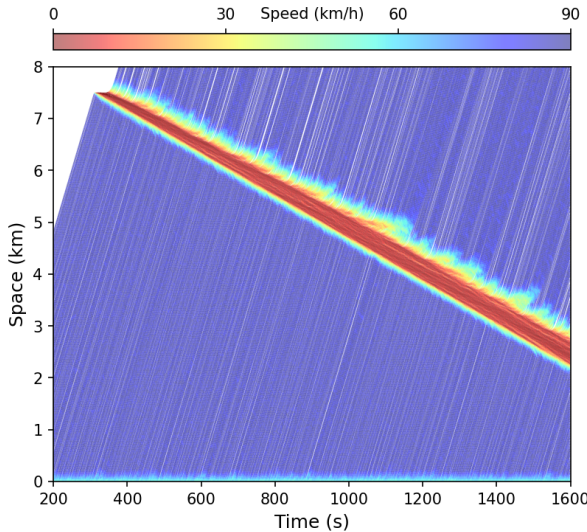


Fig. 10. SUMO simulated self-sustaining stop-and-go wave.

B. Estimation of JAD Parameters

Through the simulation scenario, we discuss and demonstrate the practical estimation of several key parameters.

1) *JAD Speed (v^*)*: As discussed in Section III-A, traffic stability is the key to estimating a reliable JAD speed that will not trigger a secondary wave. For the purpose of JAD strategy demonstration, we determine here, through simulation, the JAD speed that avoids triggering a secondary wave. As noted previously, more empirical studies and results are still needed to advance understanding of traffic stability in practice.

We reduce the speed of the first vehicle to 30, 40, 50, and 60 km/h, respectively, and simulate each scenario to

observe which speeds do not trigger secondary waves. As shown in Figure 11, speeds of 30 and 40 km/h result in traffic breakdown, and are therefore unsuitable as JAD speeds. In contrast, speeds of 50 km/h or higher can serve as reliable JAD speeds. However, as discussed in Section IV-A, increasing the JAD speed also increases the time and space required to execute the JAD task, implying a longer operational period.

Therefore, in this simulation scenario, we set the JAD speed to $v^* = 55$ km/h.

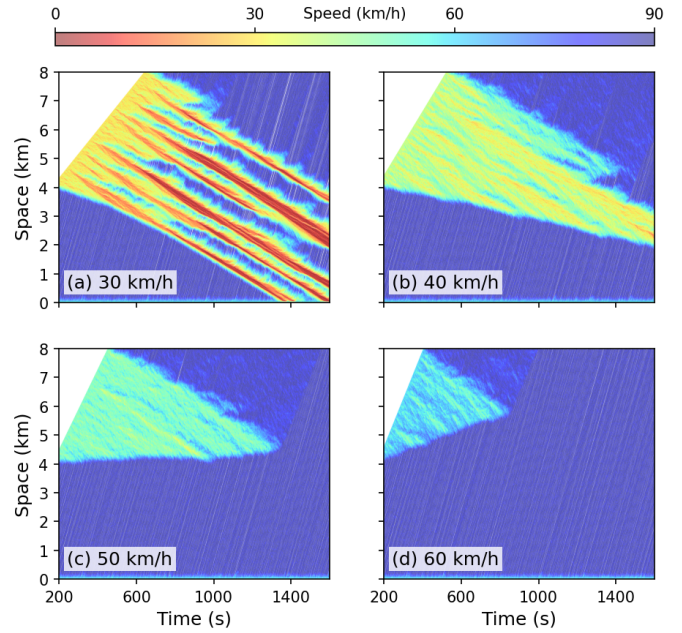


Fig. 11. Comparison of traffic breakdown under moving bottlenecks with different speeds. (a)(b) traffic breakdown; (c)(d) no breakdown.

2) *Wave temporal width (Δ_w)*: To mimic real-world conditions, we estimate the growth of a stop-and-go wave from the perspective of a stationary roadside detector.

Typically, a stationary detector monitors the traffic and measures the speed of passing vehicles in real time. Therefore, we assume that a stop-and-go wave has formed when the observed speed falls below a certain threshold and continues to remain low for a period of time. This approach is feasible because the target of this study is an isolated stop-and-go wave. In contrast, for periodic stop-and-go waves generated by fixed bottlenecks, this method may not be suitable, and the proposed JAD strategy is not designed for such traffic waves.

In this scenario, we set the threshold to 36 km/h and the holding period to 30 s. As shown in Figure 12, the resulting time-space points F and E effectively capture the stop-and-go wave. It is also noted that, due to the asymmetric behavior of vehicles traversing a stop-and-go wave [30]–[32], the recovery process from a slowly moving queue is longer than the deceleration process. As will be demonstrated later in Section V-C with simulation results, a slight overestimation of the wave speed, while probably sacrificing some efficiency, not only does not compromise the goal of halting the propagation of the stop-and-go wave, but may also improve the robustness of the JAD strategy. If one truly wants to avoid generating such

an artificial gap in traffic flow, a more advanced strategy such as the two-step strategy proposed in [12] can be adopted. However, it should be noted that more real-time traffic information is typically required to support such fine-grained management.

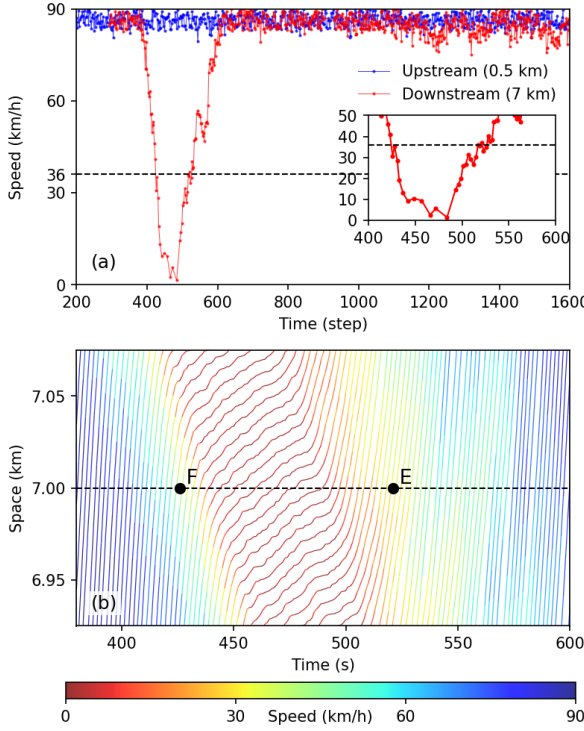


Fig. 12. Estimation of wave temporal width using a stationary roadside detector. (a) Time series of detected vehicle speed; (b) Time-space trajectories around the wave.

3) *In-wave Speed (Δ_w)*: From the practical perspective of a stationary roadside detector, the speed variation through a stop-and-go wave exhibits a gradual decrease followed by a gradual increase (also illustrated in Figure 12). As a result, the stationary roadside detector may be unable to accurately capture the in-wave speed.

Here, we take the average speed between t_F and t_E as the in-wave speed Δ_w . If the minimum value were used instead, Δ_w could be underestimated.

4) *Wave Speed (w)*: Although it is difficult to determine the specific speed of an upcoming wave using a single stationary roadside detector, it can be reasonably assumed to be prior knowledge in practice for the following two reasons. First, global empirical data have shown that wave speeds typically range from -20 to -10 km/h, indicating a relatively narrow range. Second, based on over one year of time-space diagrams of trajectories provided by the I-24 MOTION dataset [33], it is safe to assume that waves occurring at the same locations travel at the same or very similar speeds. Therefore, wave speed can be treated as prior knowledge.

Here, from the simulation, we set the wave speed to $w = -15$ km/h.

5) *Inflow Speed v_t* : The determination of the inflow speed in practice is straightforward. It can be obtained either from an upstream stationary roadside detector or from the observation of the JAD vehicle driver.

Here, we set the inflow speed v_t to be that of the potential leading vehicle, i.e., we assume that the driver of the JAD vehicle can observe this speed.

6) *The Role of the Upstream Detector*: The upstream detector provides two pieces of important information. First, it measures the inflow rate, which is critical for determining whether the current stop-and-go wave is self-sustaining. If the inflow is observed to decrease, dispatching a JAD vehicle may not be necessary, as the stop-and-go wave might dissipate naturally. Second, it provides the inflow speed, which is useful for determining the speed v_t in determining the JAD plan, as described above.

7) *Opportunity of Dispatching a JAD Vehicle*: Inserting a new vehicle into traffic requires sufficient space. Here, we propose monitoring the time headway at the standby location of the JAD vehicle. When a specified condition is satisfied, we assume that it is feasible for the JAD vehicle to merge into traffic.

In the police-car swerving scenario, the police officer is expected to identify an appropriate gap for merging. If merging from an on-ramp, the overall process would be as natural as typical daily freeway merging behavior. With the siren activated, the required gap may be even smaller than that under normal conditions.

In this study, we assume that a JAD vehicle can merge into traffic when the time headway exceeds 3 s. In simulation, we also tested smaller thresholds, such as 2 s, and found that they do not significantly disturb traffic. One reason is that, at point A, the JAD vehicle can merge at a relatively high speed (such as merging from an on-ramp), close to the prevailing traffic speed or the speed of the potential leading vehicle.

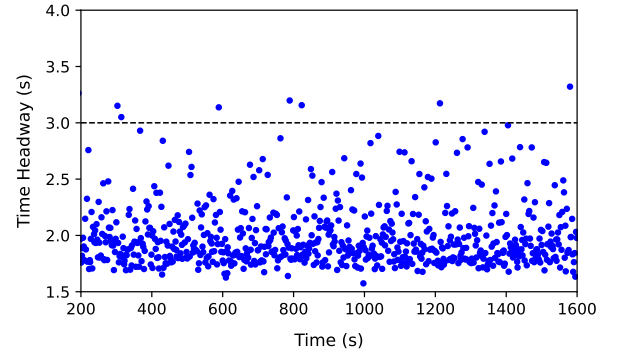


Fig. 13. Time headways at the JAD vehicle's standby location.

C. Simulation Results

To moderate multi-lane traffic, swerving behavior is required. Since such behavior has already been observed in the real world (Figure 1), it is unnecessary to simulate or verify its feasibility. Therefore, we focus on evaluating the stop-and-go mitigation effect of the JAD strategy rather than the specific swerving maneuvers of a JAD vehicle.

Figure 14 presents the simulation results. It illustrates the JAD plan (points A, B, C, D, E, and F) as well as the feasible region of point A. The results clearly show that the proposed

JAD strategy successfully suppresses the propagation of the stop-and-go wave, particularly with no triggering of secondary waves.

Meanwhile, we observe that a gap appears after the JAD vehicle completes the implementation at point C . From the perspective of suppressing stop-and-go wave propagation, having point C located slightly farther from point D does not pose a significant issue. This is a positive indication, as a conservative (slightly overestimated) choice of point C does not degrade performance, implying a good robustness of the JAD strategy.

The results could be further improved by fine-tuning the parameters. For example, a more accurate estimation of the wave width could enhance efficiency by enabling a better prediction of the ending point C of the JAD strategy. However, this refinement may not be easy to implement, because, in practice, traffic conditions cannot be perfectly replicated, and obtaining an exact value is challenging.

Note that it is not necessary to compare travel time or emissions with the baseline in Figure 10, since once the stop-and-go wave is suppressed, the following vehicles naturally experience shorter travel times and lower emissions when operating under smoother traffic conditions without falling into a stop-and-go process.

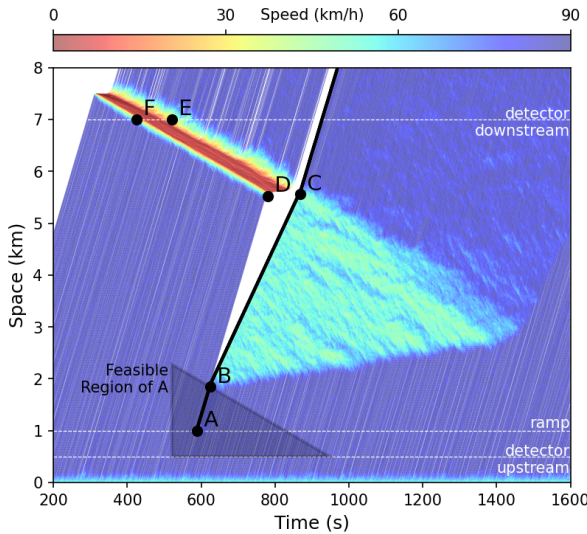


Fig. 14. A stop-and-go wave is successfully suppressed using a JAD strategy with a JAD speed of 55 km/h.

Figure 15 presents two typical cases in which the JAD vehicle fails to suppress the stop-and-go wave, as a secondary wave is triggered. In Figure 15(a), the JAD speed is set to $v^* = 35$ km/h. As indicated by the stability test in Figure 11, such a low speed is insufficient to prevent traffic breakdown. In Figure 15(b), we underestimate the wave width intentionally, and the JAD vehicle fails to avoid being captured by the stop-and-go wave. As a result, the stop-and-go wave penetrates the JAD trajectory and continues to propagate upstream.

VI. CONCLUSION

Inspired by real-world observations of police-car swerving behavior, this paper proposes a practical JAD strategy

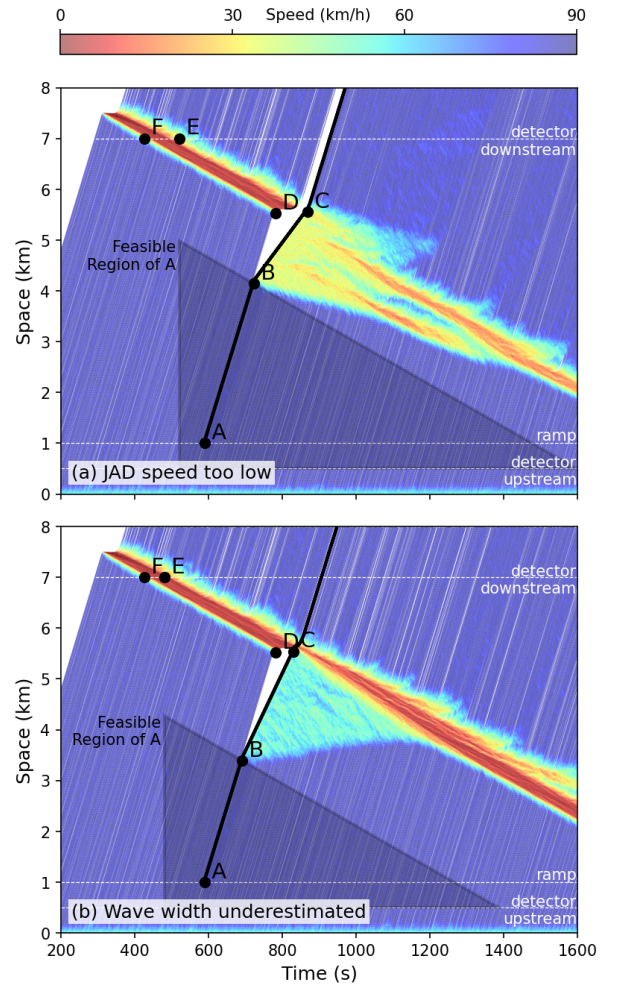


Fig. 15. A JAD strategy that fails to suppress a stop-and-go wave. (a) JAD speed $v^* = 35$ km/h is too low to prevent traffic breakdown; (b) point C is located too close to point D to effectively suppress the stop-and-go wave.

that transforms such actual behavior into a JAD maneuver capable of suppressing the propagation of an isolated stop-and-go wave. Five key parameters that significantly affect the JAD strategy, namely, *JAD speed*, *inflow traffic speed*, *wave temporal width*, *wave speed*, and *in-wave speed*, are systematically analyzed and discussed, by identifying their relative importance, characterizing their linear and nonlinear effects, and determining the direction of their influence on the JAD process (Table II). We further demonstrate that, within typical parameter ranges (Table I), the JAD behavior is feasible in practice, as the entire process typically lasts only 30~160 s and spans approximately 1~13 km (Figure II). Using a SUMO simulation as an illustrative example, we demonstrate and discuss how these parameters can be measured in practice with two stationary roadside traffic detectors. The results show that the proposed JAD strategy successfully suppresses the propagation of a stop-and-go wave, particularly without triggering secondary waves.

Among these parameters, determining an appropriate JAD speed that does not trigger traffic breakdown remains challenging in practice. This issue requires further advances in

traffic-flow stability research, particularly empirical studies. Nevertheless, this limitation does not prevent the practical implementation of the proposed JAD strategy. In practice, a relatively higher JAD speed can be adopted: based on our experience and as demonstrated in this paper, speeds such as 50 km/h or even 70 km/h (as exhibited by police-car swerving behavior in the real world shown in Figure 1) are likely to be feasible.

Learning lessons from SPECIALIST [20], [21], to ensure effectiveness and avoid unintended disturbances to the traffic system, it is essential to verify or predict, prior to dispatching a JAD vehicle, that the observed stop-and-go wave satisfies the required conditions. Specifically, the wave should be an isolated wave propagating downstream, rather than periodic oscillations associated with a fixed-location bottleneck. In short, a JAD vehicle should be dispatched only when a qualifying isolated stop-and-go wave is detected.

Overall, we believe that the present analysis substantially advances JAD studies from a purely theoretical concept toward practical application. In particular, we propose leveraging police-car swerving behavior to implement JAD, avoiding the common assumption in many previous studies that CAVs are required. While CAVs are often assumed in theoretical research nowadays, in reality, fully controllable vehicles that can participate in everyday traffic management are still rarely seen. With the proposed JAD strategy incorporating various practical considerations, the next step is real-world testing.

ACKNOWLEDGEMENT

We would like to thank Dr. Andreas Hegyi at TU Delft for sharing his valuable insights and practical experience with Variable Speed Limits and SPECIALIST, which helped inspire the ideas behind this paper.

REFERENCES

- [1] M. Yildirimoglu and N. Geroliminis, "Experienced travel time prediction for congested freeways," *Transportation Research Part B: Methodological*, vol. 53, pp. 45–63, 2013.
- [2] Z. Zhang, Y. Wang, P. Chen, Z. He, and G. Yu, "Probe data-driven travel time forecasting for urban expressways by matching similar spatiotemporal traffic patterns," *Transportation Research Part C: Emerging Technologies*, vol. 85, no. October, pp. 476–493, 2017.
- [3] L. Li, R. Jiang, Z. He, X. M. Chen, and X. Zhou, "Trajectory data-based traffic flow studies: A revisit," *Transportation Research Part C: Emerging Technologies*, vol. 114, pp. 225–240, 2020.
- [4] H. Jiang, K. Xia, Y. Zhao, Z. Yao, Y. Jiang, and Z. He, "Environmental impacts and emission reduction methods of vehicles equipped with driving automation systems: An operational-level review," *Transportation Research Part C: Emerging Technologies*, vol. 173, no. December 2024, p. 104996, 2025.
- [5] C. Wang, M. A. Quddus, and S. G. Ison, "Impact of traffic congestion on road accidents: A spatial analysis of the m25 motorway in england," *Accident Analysis & Prevention*, vol. 41, no. 4, pp. 798–808, 2009.
- [6] X. Wang, Y. Su, Z. Zheng, and L. Xu, "Prediction and interpretive of motor vehicle traffic crashes severity based on random forest optimized by meta-heuristic algorithm," *Helion*, vol. 10, no. 16, p. e35595, 2024.
- [7] W. Beaty, "Traffic "experiments" and a cure for waves & jams," 1998, accessed: 2025-04-10. [Online]. Available: <http://trafficwaves.org/trafexp.html>
- [8] ———, "Traffic waves frequently-asked questions," accessed: 2025-04-10. [Online]. Available: <http://trafficwaves.org/faq.html>
- [9] R. Nishi, A. Tomoeda, K. Shimura, and K. Nishinari, "Theory of jam-absorption driving," *Transportation Research Part B: Methodological*, vol. 50, pp. 116–129, 2013.
- [10] Y. Taniguchi, R. Nishi, T. Ezaki, and K. Nishinari, "Jam-absorption driving with a car-following model," *Physica A: Statistical Mechanics and its Applications*, vol. 433, pp. 304–315, 2015.
- [11] R. Nishi, "Theoretical conditions for restricting secondary jams in jam-absorption driving scenarios," *Physica A: Statistical Mechanics and its Applications*, vol. 542, p. 123393, 2020.
- [12] Z. He, L. Zheng, L. Song, and N. Zhu, "A jam-absorption driving strategy for mitigating traffic oscillations," *IEEE Transactions on Intelligent Transportation Systems*, vol. 18, no. 4, pp. 802–813, 2017.
- [13] K. Jerath, V. V. Gayah, and S. N. Brennan, "Influential subspaces of connected vehicles in highway traffic," *Transportation Research Circular*, vol. E-C197, pp. 151–160, 2015, transportation Research Board.
- [14] Y. Han, H. Yu, Z. Li, C. Xu, Y. Ji, and P. Liu, "An optimal control-based vehicle speed guidance strategy to improve traffic safety and efficiency against freeway jam waves," *Accident Analysis & Prevention*, vol. 163, p. 106429, 2021.
- [15] S. Li, D. Yanagisawa, and K. Nishinari, "A jam-absorption driving system for reducing multiple moving jams by estimating moving jam propagation," *Transportation Research Part C: Emerging Technologies*, vol. 158, p. 104394, 2024.
- [16] Y. Zheng, G. Zhang, Y. Li, and Z. Li, "Optimal jam-absorption driving strategy for mitigating rear-end collision risks with oscillations on freeway straight segments," *Accident Analysis & Prevention*, vol. 135, p. 105367, 2020.
- [17] S. Wang, Z. Li, Z. Cao, A. Jolfaei, and Q. Cao, "Jam-absorption driving strategy for improving safety near oscillations in a connected vehicle environment considering consequential jams," *IEEE Intelligent Transportation Systems Magazine*, vol. 14, no. 2, pp. 41–52, 2022.
- [18] Z. He, J. Laval, Y. Han, A. Hegyi, R. Nishi, and C. Wu, "A review of stop-and-go traffic wave suppression strategies: Variable speed limit vs. jam-absorption driving," *IEEE Transactions on Intelligent Transportation Systems*, p. in print, 2026.
- [19] A. Carpenter, "Cop car swerving across freeway," 2014, accessed: 2025-03-23. [Online]. Available: https://www.youtube.com/watch?v=_IvmWaSDorg
- [20] A. Hegyi, S. Hoogendoorn, M. Schreuder, H. Stoelhorst, and F. Viti, "Specialist: A dynamic speed limit control algorithm based on shock wave theory," in *2008 11th International IEEE Conference on Intelligent Transportation Systems*, 2008, pp. 827–832.
- [21] A. Hegyi and S. P. Hoogendoorn, "Dynamic speed limit control to resolve shock waves on freeways - Field test results of the SPECIALIST algorithm," in *IEEE Conference on Intelligent Transportation Systems, Proceedings, ITSC*, 2010, pp. 519–524.
- [22] M. Mauch and M. Cassidy, "Freeway traffic oscillations: observations and predictions," *15th International Symposium of Transportation and Traffic Theory*, pp. 653–673, 2002.
- [23] J. Laval and L. Leclercq, "A mechanism to describe the formation and propagation of stop-and-go waves in congested freeway traffic," *Philosophical transactions. Series A, Mathematical, physical, and engineering sciences*, vol. 368, no. 1928, pp. 4519–41, oct 2010.
- [24] Z. Zheng, S. Ahn, D. Chen, and J. Laval, "Freeway traffic oscillations: Microscopic analysis of formations and propagations using Wavelet Transform," *Transportation Research Part B: Methodological*, vol. 45, no. 9, pp. 1378–1388, nov 2011.
- [25] R. Jiang, M.-B. Hu, H. M. Zhang, Z.-Y. Gao, B. Jia, Q.-S. Wu, B. Wang, and M. Yang, "Traffic experiment reveals the nature of car-following," *PloS one*, vol. 9, no. 4, p. e94351, jan 2014.
- [26] Z. He, L. Zheng, and W. Guan, "A simple nonparametric car-following model driven by field data," *Transportation Research Part B: Methodological*, vol. 80, no. 2015, pp. 185–201, 2015.
- [27] D. Helbing and A. Greiner, "Modeling and simulation of multilane traffic flow," *Phys. Rev. E*, vol. 55, pp. 5498–5508, May 1997.
- [28] M. Treiber, A. Kesting, and R. E. Wilson, "Reconstructing the Traffic State by Fusion of Heterogeneous Data," *Computer-Aided Civil and Infrastructure Engineering*, vol. 26, no. 6, pp. 408–419, 2011.
- [29] T. Vranken and M. Schreckenberg, "Modelling multi-lane heterogeneous traffic flow with human-driven, automated, and communicating automated vehicles," *Physica A: Statistical Mechanics and its Applications*, vol. 589, p. 126629, 2022.
- [30] D. Chen, J. Laval, S. Ahn, and Z. Zheng, "Microscopic traffic hysteresis in traffic oscillations: A behavioral perspective," *Transportation Research Part B: Methodological*, vol. 46, no. 10, pp. 1440–1453, dec 2012.
- [31] L. Li, X. Chen, and Z. Li, "Asymmetric stochastic Tau Theory in car-following," *Transportation Research Part F: Traffic Psychology and Behaviour*, vol. 18, pp. 21–33, 2013.

- [32] M. Park, Y. Kim, and H. Yeo, "Development of an Asymmetric Car-Following Model and Simulation Validation," *IEEE Transactions on Intelligent Transportation Systems*, pp. 1–12, 2019.
- [33] J. Ji, A. Richardson, D. Gloudemans, G. Zachár, M. Nice, W. Barbour, J. Sprinkle, B. Piccoli, and D. B. Work, "Stop-and-go wave super-resolution reconstruction via iterative refinement," *Transportation Research Part C: Emerging Technologies*, vol. 180, p. 105313, 2025.



Zhengbing He (M'17-SM'20) received the Bachelor of Arts degree in English language and literature from Dalian University of Foreign Languages, China, in 2006, and the Ph.D. degree in systems engineering from Tianjin University, China, in 2011. He was a Post-Doctoral Researcher and an Assistant Professor with Beijing Jiaotong University, China. From 2018 to 2022, he was a Full Professor with Beijing University of Technology, China. Presently, he is a Research Scientist with the Laboratory for Information and Decision Systems (LIDS), Massachusetts Institute of Technology, USA.

His research lies at the intersection of urban mobility, systems engineering, and artificial intelligence, spanning from traditional topics such as traffic flow operations and control, sustainability, and resilience to emerging areas including data-driven modeling, autonomous driving, and large language models. In particular, he is a pioneer and long-term contributor in AI-based transportation modeling and AV-empowered traffic congestion mitigation, and an early innovator in generative AI applications in transportation

He has published more than 180 papers, with total citations exceeding 7,000 and H-index of over 40. He was listed as the World's Top 2% Scientists, ranking 67th out of over 30,000 researchers in the field of Logistics and Transportation. He is the Editor-in-Chief of the Journal of Transportation Engineering and Information (Chinese). Meanwhile, he serves as a Senior Editor for IEEE TRANSACTIONS ON INTELLIGENT TRANSPORTATION SYSTEMS, an Associate Editor for IEEE TRANSACTIONS ON INTELLIGENT VEHICLES, a Deputy Editor-in-Chief of IET Intelligent Transport Systems, and an Editorial Advisory Board Member for Transportation Research Part C. His webpage is <https://www.GoTrafficGo.com>.